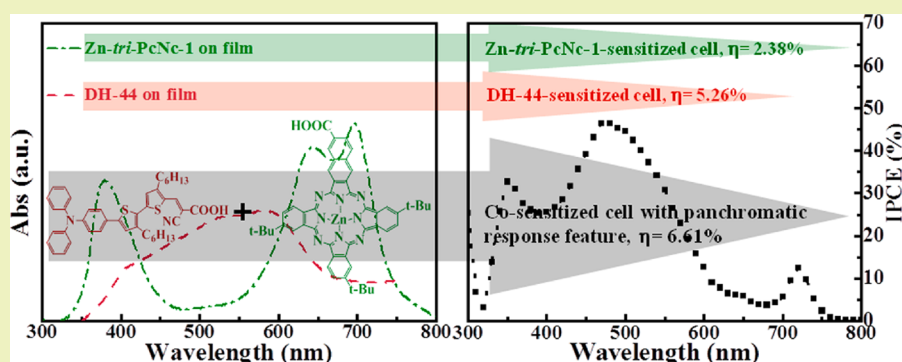


# Efficient Panchromatic Light Harvesting with Co-Sensitization of Zinc Phthalocyanine and Bithiophene-Based Organic Dye for Dye-Sensitized Solar Cells

Lijuan Yu, Ke Fan, Tainan Duan, Xingguo Chen, Renjie Li,\* and Tianyou Peng\*

College of Chemistry and Molecular Science, Wuhan University, Wuhan 430072, P. R. China



**ABSTRACT:** Co-sensitization by using two or more dyes with complementary absorption spectra as sensitizers of a semiconductor to expand the spectral response range of dye-sensitized solar cells (DSSCs) is an effective approach to enhance device performance. To improve the light-harvesting capability in the near-infrared (IR) region, zinc phthalocyanine (Zn-*tri*-PcNc-1) was applied to combine with a D- $\pi$ -A triarylamine–bithiophene–cyanoacrylate-based organic dye (DH-44) for fabrication of a co-sensitized solar cell. The resulting co-sensitized device shows an efficient panchromatic spectral response feature in the range of 320–750 nm and gives an overall conversion efficiency of 6.61%, which is superior to that of the individual dye-sensitized solar cells under standard AM 1.5G one sun irradiation. The above results represent a clear advance toward efficient and low-cost co-sensitized solar cells with a panchromatic spectral response.

**KEYWORDS:** Dye-sensitized solar cell, Co-sensitization, Spectral response, dye

## INTRODUCTION

Dye-sensitized solar cells (DSSCs) have attracted intense research due to their low cost and relatively high energy conversion efficiency.<sup>1–9</sup> For many years, the ruthenium (Ru)-bipyridyl dye families such as N719, N3, and C101 have dominated the highly efficient solar cells. However, it is well known that the above Ru-bipyridyl dyes are highly efficient only at wavelengths < 550 nm, and their spectral response falls dramatically beyond 650 nm, which results in an insufficient light harvest of near-IR light and limits conversion efficiency. Moreover, the cost and environmental issues of Ru-bipyridyl dyes are unfavorable for the application of DSSCs due to the noble metal Ru and toxicity. Therefore, many attempts, such as replacing Ru-bipyridyl dyes with metal-free organic dyes,<sup>6,7</sup> porphyrins (Pors), or phthalocyanines (Pcs),<sup>8,9</sup> have been made to expand the spectral response range and lower the device cost.

Among Ru-bipyridyl dye alternatives, metal-free organic dyes with diverse molecular structures can be easily designed and synthesized, and their molar extinction coefficients are usually higher than that of Ru-bipyridyl dyes. Moreover, organic dyes are also superior to noble metals considering cost and environmental issues.<sup>8,9</sup> Nevertheless, most organic dyes are

also not capable enough to absorb light beyond 650 nm. This insufficient absorption of deep red/near-IR light also makes organic dye-sensitized solar cells less efficient. Usually, porphyrins (Pors) and phthalocyanines (Pcs) exhibit intense spectral response bands in the near-IR region and provide good potential candidates for expanding the light responsive range of DSSCs beyond 650 nm. For example, Grätzel and co-workers reported a Por-sensitized solar cell with an overall conversion efficiency over 12%,<sup>10</sup> indicating an alternative to the noble Ru-bipyridyl dyes, while the efficiencies of most Pc-sensitized solar cells are still relatively low (about 3%). Nevertheless, Pcs possessing intense Q-band (~700 nm) absorption and promising photoelectrochemical properties are still of interest to use as near-IR dyes for DSSCs.

Recently, two or more dyes (black dye, SQ1, D131, and porphyrin) have been used for the co-sensitization of solar cells.<sup>11–13</sup> However, the co-sensitization using Pcs as the sensitizer has often resulted in an unimpressive or even lower conversion efficiency than those of single dye-sensitized solar cells.<sup>14</sup> To challenge this target, some novel ZnPc derivatives

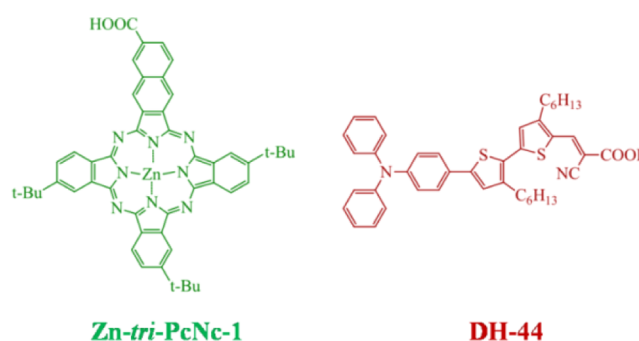
Received: October 7, 2013

Published: January 16, 2014

such as the PcSx series of dyes containing electron-donating methoxy groups with peripheral 2,6-diphenylphenol units<sup>15</sup> and zinc carboxyphthalocyanine (TT1) with a carboxy group and three *tert*-butyl (*t*Bu) groups linked directly to the Pc ring<sup>16</sup> have been developed to modify the co-sensitization with organic dyes. The presences of methoxy or *t*Bu groups not only minimized the formation of molecular aggregates but also increased the solubility of Pcs.<sup>15,16</sup> By combining PcS15 with red or orange organic dyes (D102 or D131) to cocktail-type solar cells, it was found that the co-sensitization of PcS15 and D131 resulted in an obvious enhancement of the photocurrent throughout the whole visible-light range, and therefore, the efficiencies of the cocktail-type PcS15/D131 (6.2%) and PcS15/D102 (5.6%) cells were significantly improved as compared to the PcS15 cell (5.3%).<sup>15</sup> Moreover, a co-sensitized solar cell using an organic dye (JK2) and TT1 showed a spectral response up to 700 nm with photon-to-electron conversion efficiency of 72% at 690 nm, which corresponds to the Q-band of TT1. The overall efficiency of the cocktail-type TTI/JK2 (7.74%) cell was significantly enhanced as compared to the JK2 (7.08%) or TT1 (3.52%) single dye-sensitized solar cell.<sup>16</sup> The above results indicate that efficient co-sensitized solar cells with extended spectral response in the near-IR region can be fabricated. Nevertheless, successful co-sensitization with Pc derivatives requires not only spectral matching but also avoiding interference between the highest occupied molecular orbital (HOMO) and the lowest unoccupied molecular orbital (LUMO) levels of the co-sensitized dyes. Therefore, it is still a challenge to find an appropriate dye to combine with Pcs for co-sensitization.

More recently, we developed an asymmetric zinc phthalocyanine (ZnPc) derivative (Zn-*tri*-PcNc-1), which contains tribenzonaphtho-condensed porphyrazine with one carboxyl and three *tert*-butyl (*t*Bu) groups based on the “push–pull” concept.<sup>17</sup> The three peripheral *t*Bu groups acting as electron-releasing groups can not only enhance the Pc’s solubility but also retard effectively the aggregates of Pc with higher steric hindrance, resulting in relative good conversion efficiency.<sup>17</sup> Moreover, we have also developed several new types of metal-free organic dyes as sensitizer for DSSCs.<sup>18–21</sup> Among those, bithiophene-based organic dyes (DH-41 and DH-44) contain a triphenylamine group as an electron donor, cyanoacrylic acid group as an electron acceptor, and  $\pi$ -linker of a 2,2′-bithiophene unit with two hexyl groups at different  $\beta$ -substituted positions. It was found that DH-44 containing two hexyl groups in the non-ortho- $\beta$  positions of each 2,2′-bithiophene linker shows broadened and red-shifted absorption with a relatively high molar extinction coefficient and photovoltaic performances due to its higher molecular coplanarity and intramolecular charge transfer (ICT) effect as compared with the other three DH dyes.<sup>21</sup> Scheme 1 shows the corresponding molecular structures of Zn-*tri*-PcNc-1 and DH-44. Herein, the above organic dye (DH-44) was combined with Zn-*tri*-PcNc-1 to co-sensitize the TiO<sub>2</sub> photoanode by a simple stepwise sensitization method by considering that the above asymmetric ZnPc with excellent near-IR absorption contains an optical window in the visible region, which allows their use in combination with DH-44 to achieve panchromatic light harvesting of the solar cell.<sup>17,21</sup> Comparing with the single dye-sensitized solar cells, the short-circuit current of the co-sensitized device can be increased significantly, resulting in impressively improved conversion efficiency due to the

**Scheme 1.** Molecular structures of Zn-*tri*-PcNc-1 and DH-44.



extended spectral response range from the UV to near-IR region.

## EXPERIMENTAL SECTION

**Synthesis of Photosensitizers.** *Preparation of Zn-*tri*-PcNc-1.* Asymmetric zinc phthalocyanine (Zn-*tri*-PcNc-1) was prepared according to our previous publication.<sup>17</sup> Typically, 6-carboxy methyl-2,3-dicyanonaphthalene (80 mg, 0.34 mmol), 4-*t*-Bu-phthalonitrile (374 mg, 2.0 mmol), and zinc acetate (222 mg, 1.0 mmol) were dispersed in butanol (10 mL), and then 1,8-diazabicyclo[5.4.0]undec-7-ene (1 mL) was added. The mixture was stirred at 100 °C under N<sub>2</sub> atmosphere for 12 h, and then the solvent was removed under reduced pressure. The resultant material was subjected to silica gel column chromatography with CH<sub>2</sub>Cl<sub>2</sub> as eluent. The second band (a greenish-blue one) contains Zn-*tri*-PcNc (2a), which was recrystallized twice from 50:50 (v/v) CH<sub>2</sub>Cl<sub>2</sub>/MeOH (30 mg, 10%).

A total of 100 mg of Zn-*tri*-PcNc (2a) was dissolved in 25 mL of methanol containing 1 g of Na. The reaction mixture was stirred at room temperature for 7 days, and then the solvent was removed under reduced pressure. The obtained material was redissolved in water, and pH was adjusted to 3.0 by using diluted HCl solution. Then Zn-*tri*-PcNc-1 was filtered and dried under reduced pressure. Yield: 98 mg, 98%. <sup>1</sup>H NMR (300 MHz, DMSO-*d*<sub>6</sub>,  $\delta$  ppm): 11.23 (s, 1H), 9.16 (s, 3H), 8.89–8.11 (m, 8H), 7.85–7.72 (m, 3H), 1.83 (s, 9H), 1.14 (s, 9H), 0.73 ppm (s, 9H). Elemental analysis calcd for C<sub>49</sub>H<sub>42</sub>N<sub>8</sub>O<sub>2</sub>Zn·2H<sub>2</sub>O: C, 67.16; H, 5.29; N, 12.79; found C, 66.97; H, 4.82; N, 12.73.

*Preparation of DH-44.* Metal-free organic dye (DH-44) was prepared according to our previous publication.<sup>21</sup> In a Schlenk tube, N,N-diphenyl-4-(4,4,5,5-tetramethyl-1,3,2-dioxaborolan-2-yl) aniline (1) (1.1 equiv), aldehyde (2–7) (1 equiv), Pd(PPh<sub>3</sub>)<sub>4</sub> (0.04 equiv), and K<sub>2</sub>CO<sub>3</sub> (8 equiv) were dissolved in a degassed mixed solvent of THF/H<sub>2</sub>O. The mixture was heated at 65 °C under an Ar atmosphere for 2 days. After the reaction, the organic phase was separated, dried over anhydrous Na<sub>2</sub>SO<sub>4</sub>, and filtered. The filtrate was evaporated to dryness and purified by silica gel column chromatography with petroleum ether/CH<sub>2</sub>Cl<sub>2</sub> (1:1) as eluent to afford target aldehyde (8–11).

A mixture of the aldehyde (8–11) (1.0 equiv), cyanoacetic acid (10.0 equiv), and ammonium acetate (0.5 equiv) was placed in a flask in acetic acid under an Ar atmosphere with heating 130 °C for 12 h. After cooling, the reaction was quenched by adding water and extracted with DCM. The organic layer was dried over anhydrous Na<sub>2</sub>SO<sub>4</sub>. After removing the solvent, the crude product was purified by silica gel column chromatograph eluted with toluene/methanol (10/1), and the target dyes were isolated as a powder. Yield: 70%. <sup>1</sup>H NMR (300 MHz, DMSO-*d*<sub>6</sub>,  $\delta$  ppm): 8.30 (s, 1H), 7.61 (d, 2H), 7.42 (s, 1H), 7.37–7.32 (m, 5H), 7.12–7.06 (m, 6H), 2.81 (t, 4H), 1.61 (br, 4H), 1.28 (br, 12H), 0.85 (m, 6H). <sup>13</sup>C NMR (75 MHz, CDCl<sub>3</sub>,  $\delta$  ppm): 168.9, 156.8, 148.3, 147.5, 145.2, 145.0, 144.7, 129.6, 129.3, 128.4, 127.3, 127.2, 126.8, 126.3, 125.0, 124.9, 123.7, 123.3, 116.4, 93.9, 31.9, 31.8, 31.5, 30.4, 29.4, 29.2, 22.8, 14.3. MS (ESI): *m/z* = 672.3. C<sub>42</sub>H<sub>44</sub>N<sub>2</sub>O<sub>2</sub>S<sub>2</sub> (*M*<sub>w</sub> = 614.82): calcd. C, 74.96; H, 6.59; N, 4.16; found C, 74.80; H, 6.77; N, 4.01.

### Preparation of TiO<sub>2</sub> Nanoparticles and Photoelectrodes.

**Preparation of TiO<sub>2</sub> Nanoparticles.** TiO<sub>2</sub> nanoparticles were synthesized by a hydrothermal method reported previously.<sup>22</sup> Typically, a quantity (125 mL) of titanium isopropoxide is added at room temperature to 750 mL of a 0.1 M HNO<sub>3</sub> solution under vigorous stirring. A white precipitate forms instantaneously. Immediately after the hydrolysis, the slurry is heated to 80 °C and stirred vigorously for 8 h to achieve peptization. Then the slurry was under hydrothermal conditions in an autoclave that was heated for 12 h at 200 °C. The obtained particles were rinsed with water and alcohol, followed by drying at 70 °C.

**Preparation of TiO<sub>2</sub> Paste and Photoelectrodes.** A total of 1.0 g of TiO<sub>2</sub> nanoparticles, 0.5 g of ethylcellulose, 5 mL of ethanol, 3.0 g of terpinol, and 0.2 mL of acetic acid were mixed by ball-milling for 12 h to obtain a homogeneous paste. A paste for a scattering layer was also prepared through the same method by using larger TiO<sub>2</sub> nanoparticles (diameter of ~200 nm). TiO<sub>2</sub> paste was spread on clean FTO glass (6 cm × 6 cm, 15–20 Ω sq<sup>-1</sup>) and heated at 500 °C for 30 min, and then a scattering layer was spread on the film and heated at 500 °C for 30 min again. The thicknesses of the TiO<sub>2</sub> nanoparticles film and the scattering layer were controlled by adhesive tape (Scotch, 50 μm) serving as spacers and measured to be ~6.7 and ~5.2 μm, respectively, by using TalyFormvS4C-3D profilometer (U.K.). The obtained bilayer film electrodes were dipped in 50 mM TiCl<sub>4</sub> solution at 70 °C for 30 min, followed by calcination at 500 °C for 30 min, and then incised into smaller pieces to obtain TiO<sub>2</sub> film with the same thickness.

By comparing the overall conversion efficiency of the corresponding fabricated solar cells, the individual sensitization and co-sensitization processes of Zn-*tri*-PcNc-1 and DH-44 on the TiO<sub>2</sub> photoanode are optimized in a preliminary experiment. Finally, it was found that the individual dye-sensitized electrodes prepared by immersing the obtained films in Zn-*tri*-PcNc-1 ethanol solution (0.05 mM) or DH-44 ethanol/THF (volume ratio 9:1) solution (0.3 mM) overnight could give the best conversion efficiency, while the co-sensitized electrode sensitized stepwise for 1 h in DH-44 solution and 3 h in Zn-*tri*-PcNc-1 solution in sequence exhibited the best efficiency. Moreover, the corresponding dye-loaded amounts on the TiO<sub>2</sub> photoanodes were estimated according to the absorbance differences (at 694 nm for Zn-*tri*-PcNc-1 or 497 nm for DH-44) between the initial dye solution and the filtered solution after the above-mentioned sensitization process by using the Beer–Lambert law.

**Fabrication of DSSCs and Measurements.** A dye-sensitized electrode was assembled in a classic sandwich-type cell. The platinum counter electrode was attached on the dye-sensitized photoanode after injection of the electrolyte solution, which consists of 0.5 M LiI, 0.05 M I<sub>2</sub>, and 0.1 M 4-*tert*-butylpyridine in 1:1 acetonitrile–propylene carbonate, into the interspaces between the photoanode and the counter electrode. The DSSC was illuminated by light with energy of 100 mW cm<sup>-2</sup> (AM1.5) from a 300 W solar simulator (Newport, 91160). A computer-controlled Keithley 2400 source meter was employed to collect the photocurrent–voltage (*J*-*V*) curves. The electrochemical impedance spectrum (EIS) measurements were carried out by applying open-circuit voltage under illumination and recorded over a frequency range of 0.05–10<sup>5</sup> Hz with ac amplitude of 10 mV. The obtained spectra were fitted with Z-View software (v2.1b, Scribner Associate, Inc.) in terms of an appropriate equivalent circuit.<sup>23</sup> The incident photon-to-current conversion efficiency (IPCE) was measured as a function of wavelength from 320 to 800 nm by using a Model QE/IPCE system (PV Measurements, Inc.).

## RESULTS AND DISCUSSION

**Dye Absorption Spectra Analyses.** Figure 1 illustrates the UV–vis absorption spectra of Zn-*tri*-PcNc-1 and DH-44 in ethanol (EtOH) solution and adsorbed on TiO<sub>2</sub> film, respectively. The absorption maximum ( $\lambda_{\max}$ ) and the corresponding molar extinction coefficient ( $\epsilon$ ) data of Zn-*tri*-PcNc-1 and DH-44 dyes are summarized in Table 1. As shown in Figure 1 and Table 1, Zn-*tri*-PcNc-1 in solution shows a Soret-band centered at ~343 nm and a Q-band at ~694 nm,

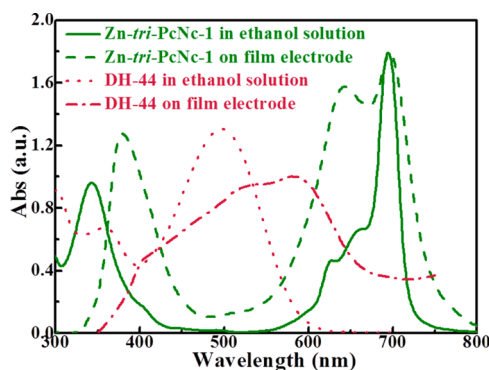


**Figure 1.** UV–vis absorption spectra of Zn-*tri*-PcNc-1 and DH-44 in solution and adsorbed on TiO<sub>2</sub> film.

while DH-44 in solution also exhibits absorption bands at two distinct spectral regions. One is at 300–400 nm that can be assigned to the localized aromatic  $\pi$ – $\pi^*$  electron transition of the conjugated molecules, and the absorption band centered at ~497 nm is attributed to an intramolecular charge transfer (ICT) process. As shown in Scheme 1, Zn-*tri*-PcNc-1 is a highly asymmetric ZnPc derivative containing tribenzonaphthocondensed porphyrazine and three *t*Bu peripheral substituent groups with high steric hindrance.<sup>17</sup> As reported in our previous investigation on a series of organic dyes (DH-41 and DH-44) with the same structural backbone,<sup>16</sup> changing  $\beta$ -substituted positions of the hexyl groups of the 2,2'-bithiophene unit can alter the molecular coplanarity, intramolecular charge transfer (ICT) effect, and spectral absorption property, and DH-44 with two hexyl groups at non-ortho- $\beta$ -substituted positions of the 2,2'-bithiophene unit has the best photovoltaic performance in its series applied in DSSCs.<sup>21</sup>

After adsorption on TiO<sub>2</sub> film, both Zn-*tri*-PcNc-1 and DH-44 show an absorption spectrum with broadened spectral response range and dramatic red-shift as compared to their respective absorption spectra of dye solution. For example, Zn-*tri*-PcNc-1 adsorbed on TiO<sub>2</sub> film shows an absorption spectrum with broadened Q-band and a dramatic red-shift of the Soret-band. The enlargement of the Q-bands may be due to the Pcs' adsorption and aggregation on the TiO<sub>2</sub> surfaces, and the red-shift of the Soret-band can be attributed to the expanded  $\pi$ -electron systems derived from the adsorbed dye coupling with TiO<sub>2</sub>.<sup>24</sup> After adsorption on TiO<sub>2</sub> film, the absorption band of DH-44 is also dramatically red-shifted as compared to the same dye in solution, as Zn-*tri*-PcNc-1 does. This should be due to the increased delocalization of the  $\pi^*$  orbital of the conjugated framework caused by the interaction between the carboxyl group and the Ti<sup>4+</sup> ions on the TiO<sub>2</sub> surfaces.

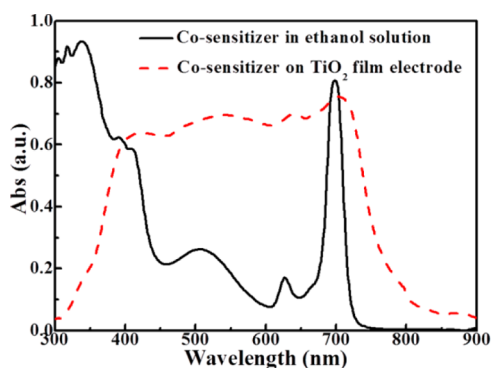
Zn-*tri*-PcNc-1 with excellent near-IR absorption contains an optical window in the visible region as shown in Figure 1, which allows its use in combination with DH-44 to obtain panchromatic spectral response. Namely, the UV–vis absorption spectra of Zn-*tri*-PcNc-1 and DH-44 match each other perfectly in either solution or on TiO<sub>2</sub> films, and therefore, it can be concluded that a combination of these two dyes in DSSCs is expected to expand the spectral absorption range and increase the light-harvesting efficiency of the solar cells. This conjecture can be further validated by the UV–vis absorption spectra of the co-sensitizers (Zn-*tri*-PcNc-1 and DH-44) in solution and adsorption on TiO<sub>2</sub> film as shown in Figure 2. The co-sensitization of the two dyes displays a highly broadened



**Table 1. Optical Properties and Electrochemical Properties of Dyes<sup>a</sup>**

dye	$\lambda_{\max}$ (nm) / $\epsilon$ ( $10^4$ M <sup>-1</sup> cm <sup>-1</sup> )	$E_{0-0}$ (eV) <sup>c</sup>	$E_{\text{ox}}$ (V) <sup>d</sup>	HOMO (eV) <sup>e</sup>	LUMO (eV) <sup>f</sup>
Zn- <i>tri</i> -PcNc-1	694/10.6	1.76	0.36	-5.07	-3.31
DH-44	497/3.56	1.96	0.78	-5.21	-3.25

<sup>a</sup>Corresponding data of Zn-*tri*-PcNc-1 and DH-44 are cited from refs 12 and 16, respectively. <sup>b</sup>Absorption maxima ( $\lambda_{\max}$ ) and corresponding molar extinction coefficient ( $\epsilon$ ). <sup>c</sup> $E_{0-0}$  is the 0–0 excitation and can be estimated from the absorption spectrum. <sup>d</sup> $E_{\text{ox}}$  is oxidation potential with reference to the ferrocene that was used as internal standard. <sup>e</sup>Calculated with the formula  $E_{\text{HOMO}} = -(E_{\text{ox}} + 4.71)$  eV. <sup>f</sup>Calculated with the formula  $E_{\text{LUMO}} = (E_{\text{HOMO}} + E_{0-0})$  eV.

**Figure 2.** UV-vis absorption spectra of the co-sensitizers (Zn-*tri*-PcNc-1 and DH-44) in solution and adsorbed on TiO<sub>2</sub> films.

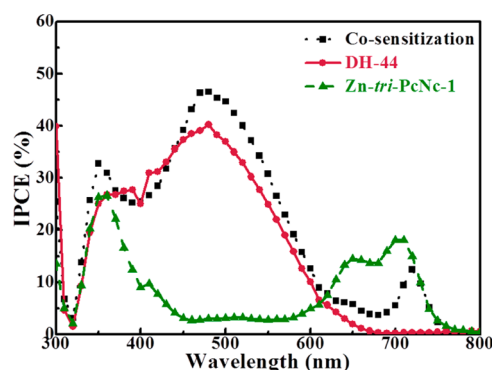
spectral response range, and the much lower absorbance in the range of 400–600 nm for the co-sensitizers solution, which is contributed by the absorption of DH-44, can be ascribed to the much lower molar extinction coefficient ( $\epsilon$ ) of DH-44 as compared to Zn-*tri*-PcNc-1 as shown in Table 1. Moreover, the co-sensitized TiO<sub>2</sub> film with two dyes shows very broad spectral absorption ranging from ~300 to 850 nm with a high absorption plateau in the range of ~400–700 nm, exhibiting a panchromatic response feature and a great potential to increase the light-harvesting efficiency of the co-sensitized solar cells.

In a preliminary experiment, the individual sensitization and co-sensitization processes of Zn-*tri*-PcNc-1 and DH-44 on the TiO<sub>2</sub> photoanode are optimized based on the measurements of the overall conversion efficiency of the fabricated solar cells, and the corresponding dye-loaded amounts on photoanodes derived from different sensitization processes are shown in Table 2. As shown, the Zn-*tri*-PcNc-1-loaded amount ( $2.78 \times 10^{-8}$  mol cm<sup>-2</sup>) on the co-sensitized photoanode is much lower than that ( $3.64 \times 10^{-8}$  mol cm<sup>-2</sup>) on the individually sensitized one although there is a similar DH-44-loaded amount between the co-sensitized ( $7.03 \times 10^{-8}$  mol cm<sup>-2</sup>) and the individually sensitized ( $7.18 \times 10^{-8}$  mol cm<sup>-2</sup>) ones. It suggests that the Zn-*tri*-PcNc-1-loaded amount is strongly influenced by the preadsorbed DH-44 on the TiO<sub>2</sub> electrode due to their competitive anchoring processes, and the differences in the dye-loaded amount would influence the photovoltaic behavior of

the co-sensitized solar cells, which will be discussed in the following sections.

### Photocurrent Density/Voltage Characteristics of DSSCs Fabricated with Different Dye-Sensitized Electrodes.

Figure 3 shows the incident photon-to-current conversion

**Figure 3.** IPCE curves of DSSCs fabricated with Zn-*tri*-PcNc-1, DH-44, and Zn-*tri*-PcNc-1/DH-44 sensitized TiO<sub>2</sub> electrode.

efficiency (IPCE) curves of DSSCs fabricated with a Zn-*tri*-PcNc-1/TiO<sub>2</sub>, DH-44/TiO<sub>2</sub>, or Zn-*tri*-PcNc-1/DH-44/TiO<sub>2</sub> electrode. As shown, the Zn-*tri*-PcNc-1-sensitized solar cell shows high IPCE in the range of 320–450 nm (corresponding to its Soret-band) and 600–750 nm (corresponding to its Q-band), while the DH-44-sensitized solar cell is effective in the range of 320–650 nm, and its corresponding IPCE values in near-IR region is relatively low. After the co-sensitization of DH-44 and Zn-*tri*-PcNc-1 in sequence, the co-sensitized solar cell exhibits effective panchromatic spectral response from UV to near-IR region in the IPCE curves. The main IPCE peak from each single dye can be significantly discovered in the IPCE curve of co-sensitized solar cell, and the spectral response of the “molecular cocktail” extends up to 750 nm, which corresponds to the Q-band of Zn-*tri*-PcNc-1. Although those IPCE values of the co-sensitized solar cell are higher than those of the individual dye-sensitized ones in the range of region of 300–620 nm, the co-sensitized cell renders lower IPCE values relative to those of the individual ZnPc-sensitized one in the region of ~620–750 nm, which corresponds to the Q-band of Zn-*tri*-PcNc-1. One possible reason for this issue may be due to

**Table 2. Photovoltaic Parameters of Solar Cells Based on Zn-*tri*-PcNc-1 and DH-44 Individually Sensitized or Co-Sensitized TiO<sub>2</sub> Electrodes**

dye	$J_{\text{sc}}$ (mA cm <sup>-2</sup> ) <sup>a</sup>	$V_{\text{oc}}$ (V) <sup>a</sup>	FF <sup>a</sup>	$\eta$ (%) <sup>a,b</sup>	dye-loaded amount (mol cm <sup>-2</sup> )
Zn- <i>tri</i> -PcNc-1	5.98	0.54	0.74	2.38 ± 0.13	$3.64 \times 10^{-8}$
DH-44	12.72	0.61	0.67	5.16 ± 0.26	$7.18 \times 10^{-8}$
co-sensitization	17.94	0.56	0.66	6.61 ± 0.35	$2.78 \times 10^{-8}$ (Zn- <i>tri</i> -PcNc-1) $7.03 \times 10^{-8}$ (DH-44)

<sup>a</sup>Data are stemmed from the corresponding typical  $J$ - $V$  curves shown in Figure 4. <sup>b</sup>Standard deviation is the calculated values based on the measurements of five parallel solar cells.

the much lower Zn-*tri*-PcNc-1-loaded amount of the co-sensitized electrode as compared with that of the individually sensitized one as mentioned above. Nevertheless, the above panchromatic spectral response including both DH-44 and Zn-*tri*-PcNc-1 spectral absorption regions indicate the effective contributions of both dyes in the co-sensitized solar cell, and its overall IPCE profile is significantly improved as compared to the single dye-sensitized one. Therefore, it should be expected that a much higher short-circuit current and better performance could be obtained from the co-sensitized solar cell, which will be discussed in the following sections.

A series of five parallel solar cells sandwiched with each kind of dyed TiO<sub>2</sub> electrode were fabricated for the photovoltaic measurements, and the typical photocurrent–voltage (*J*-*V*) and dark current curves of DSSCs fabricated with Zn-*tri*-PcNc-1/TiO<sub>2</sub>, DH-44/TiO<sub>2</sub>, or Zn-*tri*-PcNc-1/DH-44/TiO<sub>2</sub> electrode under AM1.5 one sun illumination (100 mW cm<sup>-2</sup>) or in dark are shown in Figure 4. The corresponding photovoltaic data,

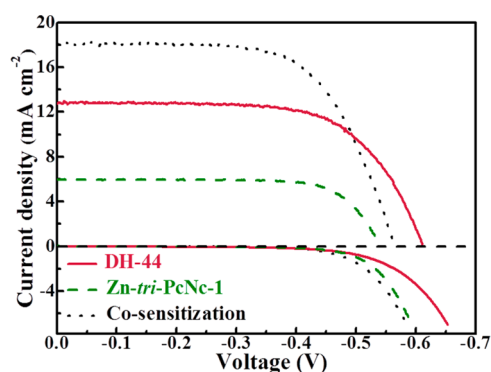


**Figure 4.** *J*-*V* curves of DSSCs fabricated with Zn-*tri*-PcNc-1, DH-44 and Zn-*tri*-PcNc-1/DH-44 sensitized TiO<sub>2</sub> electrode under 100 mW cm<sup>-2</sup> light irradiation and in the dark (bottom portion, scan rate is 10 mV s<sup>-1</sup>).

such as conversion efficiencies ( $\eta$ ), short-circuit current ( $J_{SC}$ ) and open-circuit voltage ( $V_{OC}$ ), are listed in Table 2. It should be noted that the standard deviation followed the conversion efficiency listed in Table 2 is the respective calculated values based on the measurements of the five parallel solar cells, while the listed  $J_{SC}$ ,  $V_{OC}$ , FF, and  $\eta$  values, which are very similar to their respective average values based on the measurements of the five parallel solar cells, are stemmed from the corresponding typical *J*-*V* curves shown in Figure 4. As shown, the

reproducibility of the efficiency was confirmed within an uncertainty of  $\pm 6\%$  by measuring five such parallel solar cells. The Zn-*tri*-PcNc-1-sensitized solar cell shows an impressive conversion efficiency of 2.38% with a  $J_{SC}$  of 5.98 mA cm<sup>-2</sup> and a  $V_{OC}$  of 0.54 V. The DH-44-sensitized solar cell gives a relatively high conversion efficiency of 5.16% with a  $J_{SC}$  of 12.71 mA cm<sup>-2</sup> and  $V_{OC}$  of 0.61 V, whereas the co-sensitized solar cell shows an overall efficiency of 6.61% with a  $J_{SC}$  of 17.94 mA cm<sup>-2</sup> and  $V_{OC}$  of 0.56 V. It is noted that the  $J_{SC}$  value is tremendously improved by the co-sensitization of Zn-*tri*-PcNc-1 and DH-44, which is in good agreement with the above IPCE curve. Because of the expanded spectral response to near-IR region, the  $J_{SC}$  of the co-sensitized solar cell is much higher than that of the single dye-sensitized ones, resulting in greatly enhanced conversion efficiency.

Unlike the  $J_{SC}$  results, the co-sensitized solar cell exhibits the largest dark current (which is slightly higher than that of the Zn-*tri*-PcNc-1-sensitized cell), and the DH-44-sensitized cell shows the lowest one. It is inexplicable that the co-sensitized solar cell shows the highest  $J_{SC}$  value but with the largest dark current. In principle, the  $J_{SC}$  and dark current values of a dye-sensitized solar cell are affected mainly by two processes:<sup>25,26</sup> (1) Electron photogeneration achieved by the electron injection from the photoexcited dye to the semiconductor, which can be maintained at a stationary rate because the reduced electrolyte species (i.e.,  $\Gamma^-$  ions), are able to regenerate the oxidized dye.<sup>25,26</sup> (2) Photo-injected electron recombination by reaction with the electrolyte-oxidized species (i.e.,  $I_2$  or  $I_3^-$ ), which is thought to be predominant in comparison with electron recapture by the oxidized dye because the regeneration of the oxidized dye by  $\Gamma^-$  is significantly faster than the charge transfer from TiO<sub>2</sub> to the oxidized dye.<sup>25,26</sup> Namely, the  $J_{SC}$  value increases by the electron photogeneration and injection that depends on the incident light intensity, dye's absorption coefficient, interfacial processes of dye/TiO<sub>2</sub> such as electron injection and transfer, and decreases by the photoinjected electron recombination (dark current). The present inconsistency in the changing trends of the  $J_{SC}$  and dark current of the co-sensitized solar cell might relate to competitive processes such as light absorption, dye excitation, and the photogenerated electron injection/recombination between the two kinds of dyes adsorbed in the co-sensitized film, which need to be further investigated.

**Photoelectrochemical Behaviors of DSSCs Fabricated with Different Dye-Sensitized Electrodes.** To further investigate the properties of Zn-*tri*-PcNc-1, DH-44, and DH-

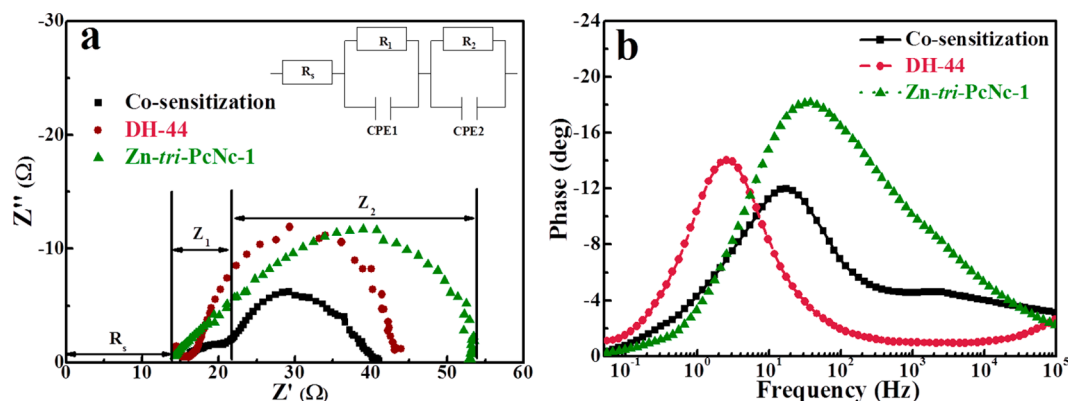


**Figure 5.** EIS spectra of DSSCs fabricated with Zn-*tri*-PcNc-1, DH-44, and Zn-*tri*-PcNc-1/DH-44-sensitized TiO<sub>2</sub> electrodes.

**Table 3. Photoelectrochemical Data of Solar Cells Based on Zn-*tri*-PcNc-1 and DH-44 Individually Sensitized or Co-Sensitized TiO<sub>2</sub> Electrodes**

dye	R <sub>s</sub> (Ω)	R <sub>1</sub> (Ω)	R <sub>2</sub> (Ω)	f (Hz)	τ <sub>n</sub> (ms)
Zn- <i>tri</i> -PcNc-1	13.56	28.47	40.52	31.50	5.06
DH-44	14.64	12.58	24.37	2.11	75.65
co-sensitization	14.62	12.71	12.71	14.36	11.09

44/Zn-*tri*-PcNc-1-sensitized TiO<sub>2</sub> electrodes, the electrochemical impedance spectra (EIS) of their respective sensitized solar cell were measured under AM1.5 one sun illumination, and their corresponding Nyquist and Bode plots<sup>23,24,27,28</sup> are shown in Figure 5a and b, respectively. Normally, a Nyquist plot features three semicircles that in the order of increasing frequency are attributed to the Nernst diffusion within the electrolyte, electron transfer at the oxide/electrolyte interface, and redox reaction at the Pt counter electrode.<sup>23</sup> In our EIS diagrams shown in Figure 5a, two obvious semicircles can be detected in the Nyquist plots. The semicircle attributed to the Nernst diffusion within the electrolyte is featureless due to the relatively fast diffusion of the electrolyte in the porous films.<sup>23,24,27</sup> Therefore, a simple equivalent circuit model, as exhibited in the inset of Figure 5a, was used to simulate the solar cells according to Kern et al.<sup>28</sup> On the basis of the model circuit for the dye-sensitized solar cell, the semicircles are assigned as shown in Figure 5a. R<sub>s</sub> represents the series resistance, which is mainly influenced by the sheet resistance of the substrate and electrical contact between FTO-glass/TiO<sub>2</sub> interfaces, R<sub>1</sub> (Z<sub>1</sub>) represents the impedance with charge transfer at the Pt counter electrode and/or electrical contact between TiO<sub>2</sub> particles, and R<sub>2</sub> (Z<sub>2</sub>) represents the impedance related to the charge transfer process at TiO<sub>2</sub>/dye/electrolyte interfaces.<sup>27,28</sup> The corresponding fitted R<sub>s</sub>, R<sub>1</sub>, and R<sub>2</sub> values for the solar cells are shown in Table 3, and R<sub>2</sub> will be discussed in detail because it relates significantly to the used dyes.

As shown in Table 3, the R<sub>2</sub> value (12.71 Ω) of the co-sensitized solar cell is greatly reduced as compared to the individual dye-sensitized ones (40.52 Ω for Zn-*tri*-PcNc-1 and 24.37 Ω for DH-44). Because R<sub>2</sub> represents the impedance related to the charge transfer process at TiO<sub>2</sub>/dye/electrolyte interfaces, it can be inferred that the charge combination rate between the injected electrons and electron acceptor (I<sub>3</sub><sup>-</sup>) in the electrolyte is lowered after the co-sensitization. As stated above, adding Zn-*tri*-PcNc-1 to a DH-44-sensitized electrode could expand the spectral response range of the solar cell from 320 to 650 nm to 320–750 nm. The light in the near-IR region can be effectively absorbed by the co-sensitized solar cell, resulting in much enhanced incident light-harvesting efficiency as reflected in IPCE curves shown in Figure 3. Because of the increased light-harvesting efficiency, more electrons can be excited from the HOMO to the LUMO energy levels of the combined dyes, and the injected rate of electrons in the dye LUMO levels to conductive band (CB) of TiO<sub>2</sub> can be accelerated. Therefore, the TiO<sub>2</sub>/dye interface resistance decreased significantly as compared to the individual dye-sensitized solar cell. Consequently, the R<sub>2</sub> value of the co-sensitized solar cell is smaller than that of Zn-*tri*-PcNc-1 or DH-44-sensitized one, which is beneficial for improving the solar cell's performance.

In the Bode plots (Figure 5b), the minor peak at the higher frequency corresponds to the charge transfer at the counter electrode. The peaks at the lower frequency are related to the charge recombination rate, and its reciprocal is regarded as

electron lifetime, τ<sub>n</sub> = 1/(2πf), where τ<sub>n</sub> and f mean the electron lifetime and frequency of superimposed ac voltage, respectively.<sup>28</sup> The obtained electron lifetimes of different solar cells are listed in Table 2 as well. As shown in Table 2, the electron lifetime (τ<sub>n</sub>) of the solar cell fabricated with Zn-*tri*-PcNc-1, DH-44-sensitized, and their co-sensitized TiO<sub>2</sub> electrodes is 5.06, 75.65, and 11.09 ms, respectively. Namely, the individual Zn-*tri*-PcNc-1 and DH-44-sensitized solar cell has the shortest and longest lifetime, respectively. This result is understandable by considering their different driving forces during the dye regeneration because dye energy levels (for instance, the LUMO level corresponds to the excited-state oxidation potential, while HOMO to the first oxidation potential) are crucial to electron injection and dye regeneration during the DSSC operations.<sup>29</sup> According to those optical and electrochemical data (Table 1) of those dyes reported in our previous literatures,<sup>17,21</sup> the energy level diagrams of Zn-*tri*-PcNc-1, DH-44, and TiO<sub>2</sub> are shown in Figure 6. As shown in Figure 6 and

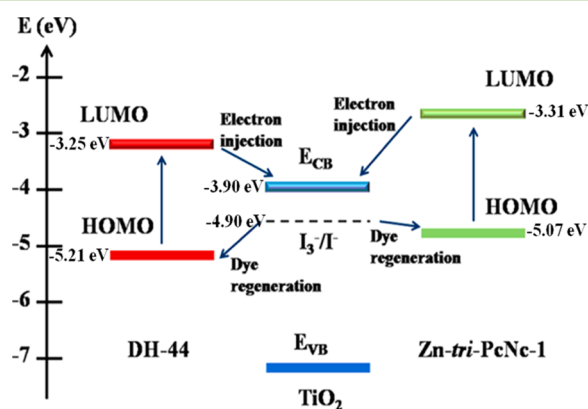
**Figure 6.** Energy level diagrams of Zn-*tri*-PcNc-1 and DH-44 dyes and TiO<sub>2</sub>.<sup>9,16</sup>

Table 1, the onset oxidative potentials of Zn-*tri*-PcNc-1 and DH-44 are around 0.36 and 0.78 V, respectively, that give the LUMO energies of those dyes around -3.31 and -3.25 eV, respectively. Both LUMO energies of those dyes are higher than the TiO<sub>2</sub> conduction band (-3.90 eV).<sup>30,31</sup> This indicates that there is sufficient driving force for the electron injection from the excited dye to TiO<sub>2</sub>. Moreover, their HOMO energies of around -5.00 eV are lower than the I<sub>3</sub><sup>-</sup>/I<sub>3</sub><sup>-</sup> potential (-4.90 eV),<sup>30</sup> suggesting that there is enough driving force for the dye's regeneration. Moreover, Zn-*tri*-PcNc-1 has a HOMO level (-5.07 eV) much closer to the energy level (-4.90 eV)<sup>25</sup> of the I<sub>3</sub><sup>-</sup>/I<sub>3</sub><sup>-</sup> shuttle than that (-5.21 eV) of DH-44, which can result in a lower driving force for the electron transfer from the I<sub>3</sub><sup>-</sup>/I<sub>3</sub><sup>-</sup> shuttle's level to the dye's HOMO during the dye regeneration. Therefore, it may be one of the hurdles for the relatively low efficiency and poor charge separation, and the reason for the shortest lifetime of Zn-*tri*-PcNc-1-sensitized solar cell. Oppositely, the DH-44-sensitized solar cell shows the longest electron lifetime due to the sufficient electron transfer



rate from  $I_3^-/I^-$  to the HOMO of DH-44 and the sufficient dye regeneration. Because the electron lifetime relates largely to the  $V_{OC}$  of the solar cells, the longer electron lifetime always leads to higher  $V_{OC}$ . Moreover, it is worth noting that the length of electron lifetimes of the solar cells in our case is in good agreement with the  $V_{OC}$  performances as shown in Table 2, i.e.,  $V_{OC}$  of the co-sensitized solar cell is reduced from 0.61 to 0.56 V as compared with the DH-44-sensitized one, while still higher than that of the Zn-*tri*-PcNc-1-sensitized one.

On the basis of the above experimental results and discussion, it can be concluded that the co-sensitization of Zn-*tri*-PcNc-1 and DH-44 dyes with complementary absorption spectra as sensitizers of semiconductor film can obtain an efficient panchromatic spectral response feature in the range of 320–750 nm of the solar cells. The light in the near-IR region can be effectively absorbed by the co-sensitized solar cell, resulting in much enhanced incident light-harvesting efficiency. Then the accelerated injection rate of the excited dye electrons to  $TiO_2$  and, therefore, the  $TiO_2$ /dye interface resistance, decreased significantly as compared to the individual dye-sensitized one, which is beneficial for improving the solar cell's performance. Apparently, the above results suggest interesting possibilities for fabricating efficient and low-cost co-sensitized solar cells with a panchromatic spectral response and high conversion efficiency.

## CONCLUSIONS

In conclusion, we have used a co-sensitized  $TiO_2$  electrode containing zinc phthalocyanine (Zn-*tri*-PcNc-1) and D- $\pi$ -A triarylamine–bithiophene–cyanoacrylate-based metal-free organic dye (DH-44) to fabricate solar cells and found that the co-sensitized solar cell exhibited a significant improvement in short-circuit current density and overall conversion efficiency (6.61%), which is much greater than that of the individual Zn-*tri*-PcNc-1 (2.38%) or DH-44 (5.16%) sensitized one. Because of the complementary absorption spectral response between Zn-*tri*-PcNc-1 and DH-44, the co-sensitized solar cell can expand the absorption spectra to about 750 nm and then enhance the short-circuit current density and overall conversion efficiency enormously. We hope the present work can provide a simple stepwise co-sensitization method to design appropriate molecules and seek more promising co-sensitized solar cells using an increased portion of the solar spectrum and providing low cost and high photovoltaic performance.

## AUTHOR INFORMATION

### Corresponding Authors

\*Telephone: +86-27-68752237. E-mail: lirj@whu.edu.cn (R.L.).

\*Telephone: +86-27-68752237. E-mail: typeng@whu.edu.cn (T.P.).

### Notes

The authors declare no competing financial interest.

## ACKNOWLEDGMENTS

This work was supported by the Natural Science Foundation of China (21271146, 21271144, and 20871096), Fundamental Research Funds for the Central Universities (2081003) of China, and Key Lab of Novel Thin Film Solar Cells (KF201111).

## REFERENCES

- (1) O'Regan, B.; Grätzel, M. A low-cost, high-efficiency solar cell based on dye-sensitized colloidal  $TiO_2$  films. *Nature* **1991**, *353*, 737–740.
- (2) Ito, S.; Nazeeruddin, M. K.; Liska, P.; Comte, P.; Charvet, R.; Pechy, P.; Jirousek, M.; Kay, A.; Zakeeruddin, S. M.; Grätzel, M. Photovoltaic characterization of dye-sensitized solar cells: Effect of device masking on conversion efficiency. *Prog. Photovolt: Res. Appl.* **2006**, *14*, 589–601.
- (3) Zhou, N.; Yang, Y. Y.; Huang, X. M.; Wu, H. J.; Luo, Y. H.; Li, D. M.; Meng, Q. B. Panchromatic quantum-dot-sensitized solar cells based on a parallel tandem structure. *ChemSusChem* **2013**, *6*, 687–692.
- (4) Hoang, S.; Ngo, T. Q.; Berglund, S. P.; Fullon, R. R.; Ekerdt, J. G.; Mullins, C. B. Improvement of solar energy conversion with Nb-incorporated  $TiO_2$  hierarchical microspheres. *ChemPhysChem* **2013**, *14*, 2270–2276.
- (5) Won, Y. S.; Yang, Y. S.; Kim, J. H.; Ryu, J. H.; Kim, K. K.; Park, S. S. Organic photosensitizers based on terthiophene with alkyl chain and double acceptors for application in dye-sensitized solar cells. *Energy Fuels* **2010**, *24*, 3676–3681.
- (6) Alibabaei, L.; Kim, J. H.; Wang, M.; Pootrakulchote, N.; Teuscher, J.; Di Censo, D.; Humphry-Baker, R.; Moser, J. E.; Yu, Y. J.; Kay, K. Y.; Zakeeruddin, S. M.; Grätzel, M. Molecular design of metal-free D- $\pi$ -A substituted sensitizers for dye-sensitized solar cells. *Energy Environ. Sci.* **2010**, *3*, 1757–1764.
- (7) Xu, S.; Zhou, C. H.; Yang, Y.; Hu, H.; Sebo, B.; Chen, B. L.; Tai, Q. D.; Zhao, X. Z. Effects of ethanol on optimizing porous films of dye-sensitized solar cells. *Energy Fuels* **2011**, *25*, 1168–1172.
- (8) Cristaldi, D. A.; Gulino, A. Functionalization of  $SnO_2$  crystals with a covalently assembled porphyrin monolayer. *ChemSusChem* **2013**, *6*, 1031–1036.
- (9) Hagfeldt, A.; Boschloo, G.; Sun, L.; Kloo, L.; Pettersson, H. Dye-sensitized solar cells. *Chem. Rev.* **2010**, *110*, 6595–6663.
- (10) Yella, A.; Lee, H.-W.; Tsao, H. N.; Yi, C.; Chandiran, A. K.; Nazeerudine, M. K.; Diao, E. W.-G.; Yeh, C.-Y.; Zakeeruddin, S. M.; Grätzel, M. Porphyrin-sensitized solar cells with cobalt (II/III)-based redox electrolyte exceed 12% efficiency. *Science* **2011**, *334*, 629–634.
- (11) Holliman, P. J.; Mohsen, M.; Connell, A.; Davies, M. L.; Al-Salihi, K.; Pitak, M. B.; Tizzard, G. J.; Coles, S. J.; Harrington, R. W.; Clegg, W.; Serpa, C.; Fontes, O. H.; Charbonneau, C.; Carnie, M. J. Ultra-fast co-sensitization and tri-sensitization of dye-sensitized solar cells with N719, SQ1 and triarylamine dyes. *J. Mater. Chem.* **2012**, *22*, 13318–13327.
- (12) Wu, H. P.; Ou, Z. W.; Pan, T. Y.; Lan, C. M.; Huang, W. K.; Lee, H. W.; Reddy, N. M.; Chen, C. T.; Chao, W. S.; Yeh, C. Y.; Diao, E. W. G. Molecular engineering of cocktail co-sensitization for efficient panchromatic porphyrin-sensitized solar cells. *Energy Environ. Sci.* **2012**, *5*, 9843–9848.
- (13) Lan, C. M.; Wu, H. P.; Pan, T. Y.; Chang, C. W.; Chao, W. S.; Chen, C. T.; Wang, C. L.; Lin, C. Y.; Diao, E. W. G. Enhanced photovoltaic performance with co-sensitization of porphyrin and an organic dye in dye-sensitized solar cells. *Energy Environ. Sci.* **2012**, *5*, 6460–6464.
- (14) Hardin, B. E.; Sellinger, A.; Moehl, T.; Humphry-Baker, R.; Moser, J.-E.; Wang, P.; Zakeeruddin, S. M.; Grätzel, M.; McGehee, M. D. Energy and hole transfer between dyes attached to titania in cosensitized dye-sensitized solar cells. *J. Am. Chem. Soc.* **2011**, *133*, 10662–10667.
- (15) Kimura, M.; Nomoto, H.; Masaki, N.; Mori, S. Dye molecules for simple co-sensitization process: Fabrication of mixed-dye-sensitized solar cells. *Angew. Chem., Int. Ed.* **2012**, *51*, 4371–4374.
- (16) Cid, J. J.; Yum, J. H.; Jang, S. R.; Nazeeruddin, M. K.; Martínez-Ferrero, E.; Palomares, E.; Ko, J.; Grätzel, M.; Torres, T. Molecular cosensitization for efficient panchromatic dye-sensitized solar cells. *Angew. Chem., Int. Ed.* **2007**, *46*, 8358–8362.
- (17) Yu, L. J.; Zhou, X. H.; Yin, Y.; Liu, Y. W.; Li, R. J.; Peng, T. Y. Highly asymmetric tribenzonaphtho-condensed porphyrinazotriazine

complex: An efficient near-IR sensitizer for dye-sensitized solar cells. *ChemPlusChem* **2012**, *77*, 1022–1027.

(18) Li, Q. Q.; Lu, L. L.; Zhong, C.; Huang, J.; Huang, Q.; Shi, J.; Jin, X.; Peng, T. Y.; Qin, J. Q.; Li, Z. Pyrrole-based organic dyes for dye-sensitized solar cells: Convenient syntheses and high efficiency. *Chem.—Eur. J.* **2009**, *15*, 9664–9668.

(19) Duan, T. N.; Fan, K.; Zhong, C.; Peng, T. Y.; Qin, J. G.; Chen, X. G. New organic dyes containing tert-butyl-capped N-arylcarbazole moiety for dye-sensitized solar cells. *RSC Adv.* **2012**, *2*, 7081–7086.

(20) Duan, T. N.; Fan, K.; Fu, Y.; Zhong, C.; Chen, X. G.; Peng, T. Y.; Qin, J. G. Triphenylamine-based organic dyes containing a 1,2,3-triazole bridge for dye-sensitized solar cells via a 'click' reaction. *Dyes Pigments* **2012**, *94*, 28–33.

(21) Duan, T. N.; Fan, K.; Zhong, C.; Chen, X. G.; Peng, T. Y.; Qin, J. G. A new class of organic dyes containing  $\beta$ -substituted 2, 2'-bithiophene unit as a  $\pi$ -linker for dye-sensitized solar cells: Structural modification for understanding relationship of structure and photovoltaic performances. *J. Power Sources* **2013**, *234*, 23–30.

(22) Barbe, C.; Arendse, F.; Comte, P.; Jirousek, M.; Lenzmann, F.; Shklover, V.; Grätzel, C. Nanocrystalline titanium oxide electrodes for photovoltaic applications. *J. Am. Ceram. Soc.* **1997**, *80*, 3157–3171.

(23) Zhao, D.; Peng, T. Y.; Lu, L. L.; Cai, P.; Jiang, P.; Bian, Z. Q. Effect of annealing temperature on the photo-electrochemical properties of DSSCs made with mesoporous TiO<sub>2</sub> nanoparticles. *J. Phys. Chem. C* **2008**, *112*, 8486–8494.

(24) Nazeeruddin, M. K.; Splivallo, R.; Liska, P.; Comte, P.; Grätzel, M. A swift dye uptake procedure for dye sensitized solar cells. *Chem. Commun.* **2003**, 1456–1457.

(25) Ito, S.; Liska, P.; Comte, P.; Charvet, R. L.; Pechy, P.; Bach, U.; Schmidt-Mende, L.; Zakeeruddin, S. M.; Kay, A.; Nazeeruddin, M. K.; Grätzel, M. Control of dark current in photoelectrochemical (TiO<sub>2</sub>/I<sup>-</sup>-I<sub>3</sub><sup>-</sup>) and dye-sensitized solar cells. *Chem. Commun.* **2005**, 4351–4353.

(26) Zaban, A.; Greenshtein, M.; Bisquert, J. Determination of the electron lifetime in nanocrystalline dye solar cells by open-circuit voltage decay measurements. *ChemPhysChem* **2003**, *4*, 859–864.

(27) Fan, K.; Gong, C. Q.; Peng, T. Y.; Chen, J. N.; Xia, J. B. A novel preparation of small TiO<sub>2</sub> nanoparticle and its application to dye-sensitized solar cells with binder-free paste at low temperature. *Nanoscale* **2011**, *3*, 3900–3906.

(28) Kern, R.; Sastrawan, R.; Ferber, J.; Stangl, R.; Luther, J. Modeling and interpretation of electrical impedance spectra of dye solar cells operated under open-circuit conditions. *Electrochim. Acta* **2002**, *47*, 4213–4225.

(29) Pei, K.; Wu, Y. Z.; Islam, A.; Zhang, Q.; Han, L. Y.; Tian, H.; Zhu, W. H. Constructing high-efficiency D-A- $\pi$ -A-featured solar cell sensitizers: A promising building block of 2,3-diphenylquinoxaline for antiaggregation and photostability. *ACS Appl. Mater. Inter.* **2013**, *5*, 4986–4995.

(30) Mack, J.; Kobayashi, N. Low symmetry phthalocyanines and their analogues. *Chem. Rev.* **2011**, *111*, 281–321.

(31) De Leeuw, D. M.; Simenon, M. M. J.; Brown, A. R.; Einerhand, R. E. F. Stability of n-type doped conducting polymers and consequences for polymeric microelectronic devices. *Synth. Met.* **1997**, *87*, 53–59.